

Performance Analysis of Reconstruction Algorithms in Diffuse Optical Tomography

K. Uma Maheswari, S. Sathiyamoorthy, G. Lakshmi

Abstract—Diffuse Optical Tomography (DOT) is a non-invasive imaging modality used in clinical diagnosis for earlier detection of carcinoma cells in brain tissue. It is a form of optical tomography which produces gives the reconstructed image of a human soft tissue with by using near-infra-red light. It comprises of two steps called forward model and inverse model. The forward model provides the light propagation in a biological medium. The inverse model uses the scattered light to collect the optical parameters of human tissue. DOT suffers from severe ill-posedness due to its incomplete measurement data. So the accurate analysis of this modality is very complicated. To overcome this problem, optical properties of the soft tissue such as absorption coefficient, scattering coefficient, optical flux are processed by the standard regularization technique called Levenberg - Marquardt regularization. The reconstruction algorithms such as Split Bregman and Gradient projection for sparse reconstruction (GPSR) methods are used to reconstruct the image of a human soft tissue for tumour detection. Among these algorithms, Split Bregman method provides better performance than GPSR algorithm. The parameters such as signal to noise ratio (SNR), contrast to noise ratio (CNR), relative error (RE) and CPU time for reconstructing images are analyzed to get a better performance.

Keywords—Diffuse optical tomography, ill-posedness, Levenberg Marquardt method, Split Bregman, the Gradient projection for sparse reconstruction.

I. INTRODUCTION

CANCER is found to be a terrible disease today which cause abnormal cell growth and it requires earlier detection to cure completely. The widely used imaging techniques [12] include Computed tomography (CT), X-ray, positron emission tomography (PET) and Magnetic resonance imaging (MRI) scan. CT scans emit a high volume of radiation. It also poses health risks to unborn babies and it is not recommended for pregnant woman. X-ray causes cell damage [13]. PET scan has a low spatial resolution. Many cancers cannot be detected via an ultrasound. The MRI scan is done in an enclosed space so the people who are fearful of being in a closely enclosed space, are facing problem with MRI. It also produces high volume of noise during the scanning process. MRI cannot be able to find all cancers and it cannot always distinguish between malignant or benign tumor, which could

K. Uma Maheswari is with Electronics and Communication Department, J.J. College of Engineering and Technology, Trichy, Tamil Nadu, India (phone: 9894491239; fax:0431-2695605; e-mail: umaragsug@gmail.com).

S. Sathiyamoorthy is with Electronics and Instrumentation Department, J.J. College of Engineering and Technology, Trichy, Tamil Nadu, India (e-mail: sathyajayam@gmail.com).

G. Lakshmi is with Electronics and Communication Department, J.J. College of Engineering and Technology, Trichy, Tamil Nadu, India (e-mail: lakshmig23@gmail.com).

lead to a false positive result. To overcome all these disadvantages, the DOT is applied. DOT is a non-invasive, functional imaging technique mainly used in bio-medical industry. It is mainly used in the early detection of sarcomas at the cellular level. It has the advantages of being non-ionizing, portable, low-cost, and this is becoming a very useful supplement to other imaging modalities like MRI, FMRI or PET scan. Optical properties of a tissue can be obtained using the principle of tomography. The DOT uses near-infrared light to probe the optical properties of human tissues such as scattering and absorption coefficient [2], [3]. This technology has attracted much attention in clinical diagnosis, for example, in breast cancer detection, monitoring of infant brain tissue oxygenation level, functional brain activation studies and cerebral hemodynamic [5]. It is a low cost alternate method for existing medical imaging technology. It involves two processes called forward problem and inverse problem.

Forward problem describes the photon propagation in tissue and used to determine the optical flux in tissue boundary. The inverse problem involves in the reconstruction of the tissue image from the absorption, scattering coefficient and optical flux of tissue, which was determined from light measurements on the phantom surface of the boundary [1]. The inverse problem is difficult to solve because of the issue of ill-posedness that is the problem fails to be well posed. The properties of well posed problems are a solution exists, the solution is unique, and the solution depends continuously on the data [6]. The third property is very important in finding the inverse problem which determines the stability of our solution. If the problem solution does not depend continuously on the data, it leads to the ill-posedness problem. Here, the small changes in the data will result in large changes in our solution. To solve this problem, regularization methods are used that is a regularization method introduced additional information in order to create a well posed data [26], [27]. Diffuse optical imaging [19]-[22] technique aims to produce the spatially resolved images and enhances the low resolution functional image with high resolution complementary structural information using for an MRI scan and X-rays. In experimental systems, a set of optical fiber was attached to the boundary of the object as measurement detectors and sources. The light source was laser sources in near-infra-red (NIR) wavelength diffuse on the phantom and the scattered rays are measured using photo-detectors [5]. In order to remove the ill-posedness, the regularization technique [21] is used among which Levenberg-Marquardt method (LM) is perhaps the most commonly used methods. After the regularization process Split Bregman reconstruction method [22]-[25] is used to

reconstruct the image of a soft tissue. The reconstruction algorithms such as Split Bregman and GPSR [28] algorithms are analyzed here provide the better reconstruction algorithm.

Bo Bi et al. [5] provide the sparsity regularization technique for image reconstruction in DOT. Gehre et al. [8] investigates the potential of sparsity constraints in the electrical impedance tomography (EIT) inverse problem of inferring the distributed conductivity based on boundary potential measurements. Chamorro et al. [15] proposes an algorithm called Algebraic reconstruction technique - Split Bregman (ART-SB), which provides the solution for L1-regularized problem. Wang et al [27] present an evaluation of the use of Split Bregman iterative algorithms for the L1-norm regularized inverse problem of electrical impedance tomography. Figueiredo et al. [28] proposes a gradient projection algorithm for the boundary constrained quadratic programming formulation of ill-conditioned problems.

The organization of the paper is as follows; Section II we discuss about the forward model using a radiative transfer equation. In Section III, the inverse model is discussed which is used to reconstruct an image of a soft tissue by evaluation of frechet derivative between the actual measured data and true data. Section IV discusses about the resultant reconstructed images of absorption and scattering coefficient and section V gives the conclusion drawn from the performance graph of image reconstruction algorithms.

II.FORWARD MODEL

The forward model of DOT is exercised to determine the light propagation through the tissue medium when the incident impulse and the absorption and scattering coefficients are known. It describes the photon propagation in tissue [14]. In the experimental procedure of acquiring potential measurements is as follows. Initially, a set of **s** laser sources and **d** detectors were placed on the boundary of the head. The incident impulse is launched from the laser source and record the resulting measurement from all the detectors. This procedure can be modelled mathematically. The Radiative Transfer Equation (RTE) [16] is used to describe the photon propagation in tissues. The RTE [17] has many advantages which include the possibility of modelling the light transport through an irregular tissue medium.

The light diffusion equation [15] in frequency domain is,

$$\begin{aligned} & \left(-\nabla \cdot k(r) \nabla + \left(\mu(r) + \frac{j\omega}{c} \right) \right) \phi(r, \omega) \\ &= [A_{dc} \delta(\omega) + A_{ac} \delta(\omega - \omega_0)] \delta(r - r_0) \end{aligned} \quad (1)$$

where $\phi(r)$ is the photon flux, $k(r)$ is the diffusion coefficient and is given by

$$k(r) = \left[\frac{1}{3(\mu_a(r) + \mu_s(r))} \right] \quad (2)$$

μ_a and μ_s are absorption coefficient and reduced scattering coefficient [20] ($\mu_a \ll \mu_s$) respectively. The input photon is from a source of constant intensity A_{dc} located at $r = r_0$ [4].

III.INVERSE MODEL

The inverse problem is used to reconstruct the image by estimating scattering and absorption coefficients [10], [11]. The actual measurement has the noise level δ ; that is $\|M_i^\delta - M_i\| \leq \delta$, where M_i^δ represents the actual measurement data and M_i represents the true data [5]. The inverse problem of DOT is to determine (μ_t, μ_s) such that the following nonlinear equation hold:

$$F_i(\mu_t, \mu_s) = M_i^\delta, \quad (\mu_t, \mu_s) \in D \quad (3)$$

For $i=1, \dots, s$. Since the inverse problem of DOT suffers from severe ill-posedness, the regularization technique [18] is used to reconstruct the image. The minimization of Tikhonov functional is:

$$J(\mu_s) := \frac{1}{2} \sum_{i=1}^s \|F_i(\mu_s) - M_i\|_{L^2(\partial X)}^2 + \alpha R(\mu_s) \quad (4)$$

Over the set,

$$Q_{ad} = \{\mu_s \in L^\infty(X)\} \quad (5)$$

for the coefficient μ_s . Here $R(\mu_s)$ is a regularization penalty function. By analyzing the minimization problem,

$$\inf_{\mu_s \in Q_{ad}} J(\mu_s) \quad (6)$$

Here we consider the standard reconstruction method.

A. Standard Reconstruction

The traditional L_2 norm squared penalty is considered to minimize the following function,

$$R(\mu_s) = \frac{1}{2} \|\nabla \mu_s\|_{L^2(X)}^2 \quad (7)$$

$$J(\mu_s) = \frac{1}{2} \sum_{i=1}^s \|F_i(\mu_s) - M_i^\delta\|_{L^2(\partial X)}^2 + \frac{\alpha}{2} \|\mu_s - \mu_s^*\|_{L^2(X)}^2 \quad (8)$$

Levenberg Marquardt [29] regularization method [7] is used in the inverse problem of DOT. For every $1 \leq i \leq s$, the forward operator is linearized around some initial guess μ_s^0 ;

$$F_i(\mu_s) = F_i(\mu_s^0) + F'_i(\mu_s^0)(\mu_s - \mu_s^0) + R(\mu_s^0; i) \quad (9)$$

where, $F'_i(\mu_s^0)$ is the frechet derivative of $F_i(\mu_s)$ and $R(\mu_s^0; i)$ denotes the Taylor remainder for the linearization around μ_s^0 . Substituting the above equation in $J(\mu_s)$ and the higher-order remainder of $R(\mu_s^0; i)$ getting ignored [8].

$$\inf_{\mu_s \in D} \frac{1}{2} \sum_{i=1}^s \|F_i(\mu_s^0) + F'_i(\mu_s^0)(\mu_s - \mu_s^0) - M_i^\delta\|_{L^2(\partial X)}^2 + \frac{\alpha}{2} \|\mu_s - \mu_s^0\|_{L^2(X)}^2 \quad (10)$$

The Euler equation of the discrete problem is

$$\sum_{i=1}^s F'_i(\mu_s^0)^* (F_i(\mu_s^0) + F'_i(\mu_s^0)(\mu_s - \mu_s^0) - M_i^\delta) + \alpha(\mu_s - \mu_s^0) = 0; \quad (11)$$

By solving (11) we can get the final resultant equation [9].

$$\left(\sum_{i=1}^s F'_i(\mu_s^0)^* F'_i(\mu_s^0) + \alpha I \right) (\mu_s - \mu_s^0) = - \sum_{i=1}^s F'_i(\mu_s^0)^* (F'_i(\mu_s^0) - M_i^\delta) \quad (12)$$

'I' is the identity matrix.

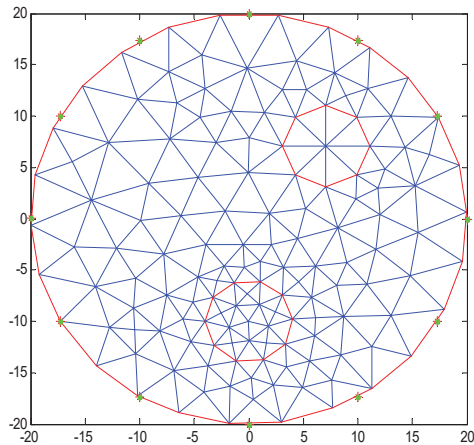


Fig. 1 Mesh diagram of inverse problem using the Split Bregman method

IV.RESULTS AND DISCUSSION

In our simulation the scattering coefficient is reconstructed with the standard regularization reconstruction algorithm. We perform the simulations on a 3.0 GHz PC with 8 GB RAM in MATLAB 2013b environment under Windows7. The boundary measurements are the excitation received by photo-detectors attached to the boundary of the tissue. The Levenberg Marquardt regularization technique and Split Bregman Reconstruction method for image reconstruction was implemented and analyzed. Fig. 1 shows the Mesh diagram for the inverse model solved using Levenberg Marquardt equation. Fig. 2 shows the actual measurement values of absorption and scattering coefficients of the normal people. Fig. 3 shows the actual measurement values of absorption and scattering coefficients of the cancer affected people. Fig. 4 provides the graph that explaining the absorption coefficient values for

normal and cancer affected people. Fig. 5 explains the range of scattering coefficient for normal and cancer affected people.

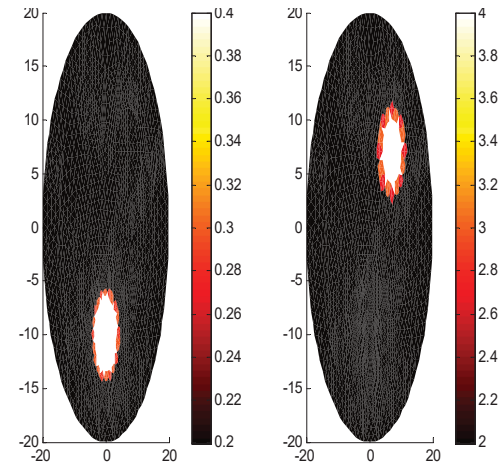


Fig. 2 Reconstructed image for Normal people

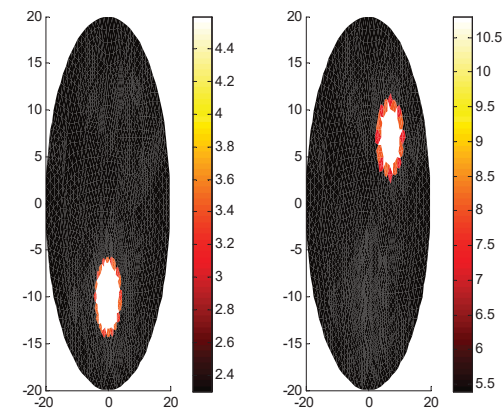


Fig. 3 Reconstructed images for Cancer affected people

TABLE I
 PREDICTION OF ABSORPTION AND SCATTERING COEFFICIENT VALUES FOR
 NORMAL AND CANCER AFFECTED PEOPLE

| Optical parameters of a human tissue | | |
|--------------------------------------|---------------------------|------------------------|
| Parameter name | Normal people | Cancer affected people |
| Absorption coefficient | 0.01 0.5 1.1 1.2 | 2 2.3 2.5 2.7 |
| Scattering coefficient | 1.3 1.8 2 2.5 | 5 5.3 6 6.5 |

Table I gives the absorption and scattering coefficient values of the normal people and cancer affected people observed from the reconstructed image. This variation was exploited in the reconstructed image; therefore, we can distinguish the normal people and the affected people as illustrated in Figs. 4 and 5. For the normal people, the absorption coefficient is less than 2 cm^{-1} and scattering coefficient values is less than 5 cm^{-1} . For the cancer affected people, the absorption coefficient is greater than 2 cm^{-1} and scattering coefficient value is greater than 5 cm^{-1} .

In the DOT reconstruction problems, the measurement data are usually synthesized from the numerical solutions of the forward problem. Here the ill-posedness of the inverse problem is removed using regularization techniques. The measurement techniques of the optical devices are very limited, so we cannot accurately receive the existence from all angles instead we receive a boundary angular averaged data.

Absorption Coefficient

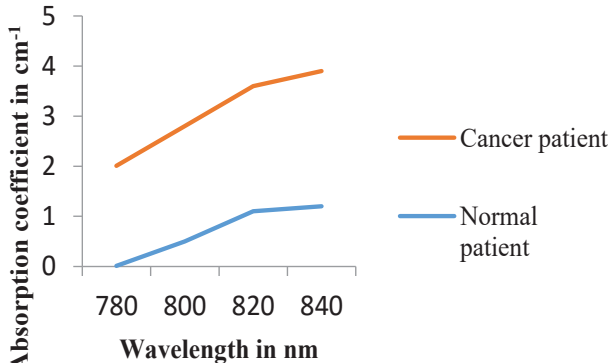


Fig. 4 Absorption coefficient distribution for normal and affected people

Scattering Coefficient

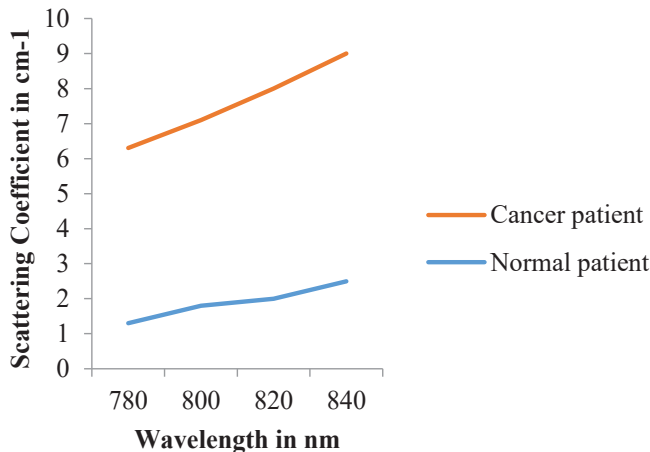


Fig. 5 Scattering coefficient distribution for normal and affected people

Our purpose is to reconstruct the scattering coefficient and the absorption coefficient which was assumed to be known. By comparing the true value with the reconstructed result we can obtain the reconstructed result. The number of nodes in the forward problem mesh is always higher than the number of nodes in reconstructing mesh. Number of nodes before the reconstruction is 1097 and after the reconstruction the number of nodes will be 286. We are able to get the values of oxygenated and deoxygenated hemoglobin values from the reconstructed image. By analyzing the above values, we can able to find the difference between the normal tissue and the cancer affected tissue. When the absorption and scattering

coefficient has higher values (above 2 cm^{-1} and above 5 cm^{-1} respectively), there is prediction of tumor as malignant or benign tumor of the soft tissue. We can reveal the resolution of the reconstructed image by calculating SNR, CNR, Relative solution error norm (RE) and CPU time. SNR is calculated as

$$SNR = 10\log_{10}\left(\frac{P_{signal}}{P_{noise}}\right) \quad (14)$$

The CNR is a measure used to determine the image quality. It is calculated using the mean and standard deviation values. CNR is calculated as

$$CNR = \frac{S_A - S_B}{\sigma_0} \quad (15)$$

where S_A, S_B are the signal intensities of the images while σ_0 is the standard deviation of the pure image noise. The Relative solution error norm is calculated as

$$RE = \frac{\|\mu_s - \mu_s^{true}\|_2}{\|\mu_s^{true}\|_2} \quad (16)$$

TABLE II
 PERFORMANCE ANALYSIS OF RECONSTRUCTION ALGORITHMS

| Parameters | Split Bregman Method | GPSR |
|--------------|----------------------|--------|
| SNR | 5.7946 | 4.9431 |
| CNR | 11.157 | 9.6832 |
| RE | 0.1124 | 0.1684 |
| CPU time (s) | 72.231 | 76.243 |

Table II compares the parameters to study the performance of reconstruction algorithms. The SNR value of the Split Bregman method is greater than the GPSR algorithm and it also has improved CNR than GPSR method. RE of a reconstructed image should be low to achieve better performance. The GPSR method provides high RE value, so it is not an optimal solution for image reconstruction. Finally Split Bregman method requires less CPU time to execute compared to GPSR method. Fig. 6 shows the graph that explains the performance analysis of both Split Bregman and GPSR algorithms.

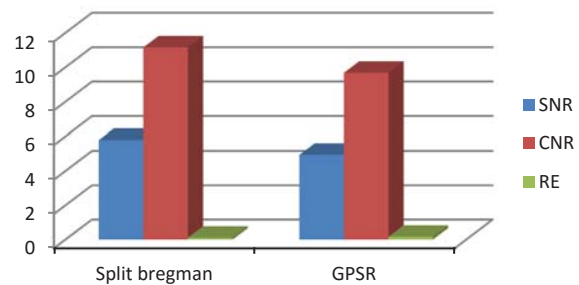


Fig. 6 Comparison of parameters of two algorithms

By comparing all the parameters in Table II, we can conclude that the Split Bregman method is simple, efficient and provides higher performance compared to GPSR. Efficient reconstruction algorithm and proper regularization techniques are essential to get high resolution images of a soft tissue and to remove the ill-posedness. Split Bregman method completely provides the linear solution and removes the ill-posedness of the inverse problem of DOT.

V.CONCLUSION

By using the reconstruction algorithms in DOT, we implemented the Levenberg-Marquardt regularization algorithm and reconstruction algorithm called Split Bregman method which is proven to be easy to reconstruct an image. The performance of the Split Bregman method is compared with the GPSR method. The Split Bregman method is predictable compared with GPSR method. The Split Bregman method performs steadily with various measurement data and it also provides practical solutions for image reconstruction. The Split Bregman method provides better performance than GPSR method. The error percentage of Split Bregman method is less than GPSR method. From the reconstructed image, absorption and scattering coefficient values are analyzed to find the difference between normal soft tissue and cancer affected tissue. One way to increase the quality of a reconstructed image is to increase the number of measurements by adding more number of photo detectors. Finally, the ill-posedness problem is removed by regularization technique and high resolution image is achieved through a Split Bregman reconstruction algorithm.

REFERENCES

- [1] S. R. Arridge, "Optical tomography in medical imaging," *Inverse Problems*, vol. 15, no. 2, pp. R41–R93, 1999.
- [2] S. R. Arridge and J. C. Schotland, "Optical tomography: forward and inverse problems," *Inverse Problems*, Vol. 25, no. 12, Article ID 123010, 2009.
- [3] A. P. Gibson, J. C. Hebden, and S. R. Arridge, "Recent advances in diffuse optical imaging," *Physics in Medicine and Biology*, Vol. 50, no. 4, article R1, 2005.
- [4] Samir Kumar Biswas, Rajan Kanhirodan, Ram Mohan Vasu, "Models and algorithms for Diffuse Optical Tomographic System", *Network and system sciences*, 6,489-496,2013
- [5] Bo Bi, Bo Han, Weimin Han, Jinping Tang and Li Li, "Image Reconstruction for Diffuse Optical Tomography Based on Radiative Transfer Equation" *computational and mathematical methods in Medicine*, volume 2015, Article ID 286161,2015
- [6] J. Nocedal and S. J. Wright, *Numerical Optimization*, Springer Series in Operations Research, Springer, New York, NY, USA, 1999.
- [7] M. Hanke, "The regularizing Levenberg-Marquardt scheme is of optimal order," *Journal of Integral Equations and Applications*, Vol. 22, no. 2, pp. 259–283, 2010.
- [8] M. Gehre, T. Kluth, A. Lippinen et al., "Sparsity reconstruction in electrical impedance tomography: an experimental evaluation", *Journal of Computational and Applied Mathematics*, Vol. 236, no. 8, pp. 2126–2136, 2012.
- [9] J. Kaipio and E. Somersalo, *Statistical and Computational Inverse Problems*, Springer, New York, NY, USA, 2005.
- [10] D. L. Colton and R. Kress, *Inverse Acoustic and Electromagnetic Scattering Theory*, Springer, Berlin, Germany, 2nd edition, 1998.
- [11] M. Jiang, T. Zhou, J. Cheng, W. X. Cong, and G. Wang, "Image reconstruction for bioluminescence tomography from partial measurement," *Optics Express*, vol. 15, no. 18, pp. 11095–11116,2007.
- [12] H. B. Jiang, *Diffuse Optical Tomography: Principles and Applications*, CRC Press, Boca Raton, Fla, USA, 1st edition, 2010.
- [13] W. Han, J. A. Eichholz, X. L. Cheng, and G. Wang, "A theoretical framework of x-ray dark-field tomography," *SIAM Journal on Applied Mathematics*, vol. 71, no. 5, pp. 1557–1577, 2011.
- [14] H. Gao, S. Osher, and H. K. Zhao, "Quantitative photo acoustic tomography," in *Mathematical Modeling in Biomedical Imaging II, Lecture Notes in Mathematics*, pp. 131–158, Springer, Berlin, Germany, 2012.
- [15] J. Chamorro-servent, J. F. P. J. Abascal, J. Aguirre, Simon Arridge, Teresa Correia, Jorge Ripoll, Manuel Desco and Juan J. Vaquero, "Use of split Bergman denoising for iterative reconstruction in fluorescence diffuse optical tomography", *Journal of Biomedical optics*, vol.18,no.7, Article ID 076016, 2013.
- [16] J. Tang, W. Han, and B. Han, "A theoretical study for RTE-based parameter identification problems," *Inverse Problems*, vol. 29, no. 9, Article ID 095002, 2013.
- [17] H. Gao and H. K. Zhao, "Analysis of a numerical solver for radiative transport equation," *Mathematics of Computation*, Vol. 82, no. 281, pp. 153–172, 2013.
- [18] R. Sukanyadevi, K. Umamaheswari, S. Sathiyamoorthy, Resolution improvement in Diffuse Optical Tomography, *International Journal of Computer Applications ICIIOES* (9), 2013.
- [19] K. Uma Maheswari, S. Sathiyamoorthy, "Soft Tissue Optical Property Extraction for Carcinoma Cell Detection in Diffuse Optical Tomography System under Boundary Element Condition", *Optik-International journal for light and electron optics*, Vol. 127 (3), 1281-1290, 2016.
- [20] K. Uma Maheswari, S. Sathiyamoorthy, "Stein's Unbiased Risk Estimate Regularization (SURE) for Diffuse Optical Tomography (DOT) System Enhances Image Reconstruction with High Contrast to Noise Ratio (CNR)", *International Journal of Applied Engineering Research*, 10 (24), 21186-21191, 2015.
- [21] Sabrina brigade, Samuel Powell, Robert J cooper et al., "Evaluating real-time image reconstruction in diffuse optical tomography using physiologically realistic test data", *Biomedical optical express*, Vol. 6, Issue 12, pp. 4719-4737 ,2015.
- [22] J. F. CAI, S. Osher, and Z. W. Shen, "Linearized Bregman iterations for compressed sensing", *Mathematics of computation*, vol. 78, no. 267, pp. 1515–1536,2009.
- [23] T. Goldstein and S. Osher, "The Split Bregman method for L1 regularized problems", *SIAM journal on imaging sciences*, Vol. 2, no. 2, pp. 323-343, 2009.
- [24] W. Yin, S. Osher, J. Durban, and D. Goldfarb, "Bregman iterative algorithms for l1 minimization with applications to compressed sensing", *SIAM journal on imaging science*, Vol. 1, no. 1, pp. 143-168, 2008.
- [25] W. T. Yin, "Analysis and generalization of the linearized Bregman model," *SIAM Journal on imaging science*, vol. 3, no. 4, pp. 856-877, 2010.
- [26] J. Bush, "Bregman algorithms", M. S. thesis, University of California, Santa Barbara, Calif, USA, 2011.
- [27] J. Wang, J. Ma, B. Han, and Q. Li, "Split Bregman iterative algorithm for sparse reconstruction of electrical impedance tomography", *Signal Processing*, Vol. 92, no. 12, pp. 2952-2961, 2012.
- [28] M. A. T. Figueiredo, R. D. Nowak, and S. J. Wright, "Gradient projection for sparse reconstruction: application to compressed sensing and other inverse problems", *IEEE journal of selected topics in Signal Processing*, Vol. 1, no. 4, pp. 586-597, 2007.
- [29] K.Umamaheswari, S.Sathyamoorthy and G.Lakshmi, "Numerical solution for image reconstruction in diffuse optical tomography", *Journal of Engineering and Applied Science*, vol.11, pp. 1332-1336.